The Plant Cell, Vol. 21: 2298–2306, August 2009, www.plantcell.org 

# *Arabidopsis* Cortical Microtubules Are Initiated along, as Well as Branching from, Existing Microtubules [W]

**Jordi Chan,[1] Adrian Sambade, Grant Calder, and Clive Lloyd**

Department of Cell and Developmental Biology, John Innes Centre, Colney, Norwich, NR4 7UH, United Kingdom

**The principles by which cortical microtubules self-organize into a global template hold important implications for cell wall patterning. Microtubules move along bundles of microtubules, and neighboring bundles tend to form mobile domains that flow in a common direction. The bundles themselves move slowly and for longer than the individual microtubules, with domains describing slow rotary patterns. Despite this tendency for colinearity, microtubules have been seen to branch off extant microtubules at ~45°. To examine this paradoxical behavior, we investigated whether some microtubules may be born on and grow along extant microtubule(s). The plus-end markers *Arabidopsis thaliana* end binding protein 1a, AtEB1a-GFP, and *Arabidopsis* SPIRAL1, SPR1-GFP, allowed microtubules of known polarity to be distinguished from underlying microtubules. This showed that the majority of microtubules do branch but in a direction heavily biased toward the plus end of the mother microtubule: few grow backward, consistent with the common polarity of domains. However, we also found that a significant proportion of emergent comets do follow the axes of extant microtubules, both at sites of apparent microtubule nucleation and at cross-over points. These phenomena help explain the persistence of bundles and counterbalance the tendency to branch.**

## INTRODUCTION

Microtubules in interphase plant cells have been seen to be associated with the plasma membrane, forming parallel groups or bundles (Hardham and Gunning, 1978; Lancelle et al., 1986; Shaw et al., 2003). These groupings represent the basic building blocks of the cortical microtubule array, and dynamic studies with fluorescently tagged microtubules show that successive microtubules grow along the same bundle over several minutes (Chan et al., 2003; Dhonukshe et al., 2005). Over still longer time periods (several hours), we recently showed that bundles undergo unsuspected rotary movements in *Arabidopsis thaliana* hypocotyl epidermal cells (Chan et al., 2007). These observations revealed intriguing but unexplained features, such as the ability of bundles to self-perpetuate and move in the direction of individual microtubule plus ends, albeit more slowly. Adjacent bundles can share the same polarity of movement, forming domains that migrate over the cortex while maintaining a shifting, branching network. Cell surfaces contain several polarized domains, and it is their ability to move in curved paths, clockwise or anticlockwise, that generates the progressive rotation of the entire microtubule array (Chan et al., 2007). Microtubules have been shown to guide the movements of cellulose synthesizing enzymes along the plasma membrane of *Arabidopsis* hypocotyl cells (Paredez et al., 2006) and so the fact that microtubule bundles undergo rotary movements themselves is likely to be fundamentally important for the organization of cellulose microfibrils in the cell wall (Giddings and Staehelin, 1991). Rotation might explain the helicoidal wall structure of hypocotyl (Refrégier et al., 2004) and stem (Hejnowicz, 2005) epidermal cells, in which cellulose microfibrils are arranged in layers that progressively change angle like the steps of a spiral staircase. Microtubule rotation may not, however, be a feature of other cells, such as elongating root cells, in which microtubules are organized in transverse alignments (Sugimoto et al., 2007).

Here, we have sought explanations for the formation of polarized domains and for the persistence of bundles composed of relatively transient microtubules that successively move along the same axes. In their study using green fluorescent protein (GFP)-tubulin, Murata et al. (2005) drew attention to the apparent paradox that although cortical microtubules have a tendency to bundle, new microtubules branch off extant microtubules. However, when labeling the entire microtubule with GFP-tubulin, it is difficult to distinguish the origins of one microtubule moving along another, causing a potential underestimate of microtubules born upon a track (Dixit et al., 2006). We therefore reexamined this problem in *Arabidopsis* seedlings by expressing the plus tip markers AtEB1a-GFP and SPR1-GFP that define the polarity of growth (Chan et al., 2003; Sedbrook et al., 2004; Dhonukshe et al., 2005; Dixit et al., 2006; Timmers et al., 2007). Knowing the polarity of the mother microtubule, it is possible to show that microtubule branching is highly biased relative to the plus end of the mother, with few microtubules growing backward toward the minus end. Furthermore, it was possible to see that a significant nonbranching population of microtubules arises upon the mother microtubule and grows along its axis to the plus end, accounting for the long-term persistence of the track as an entity. The data also show that new microtubules arise where microtubules cross and follow one of the crossing axes. So although

[1] Address correspondence to jordi.chan@bbsrc.ac.uk.

The author responsible for distribution of materials integral to the findings presented in this article in accordance with the policy described in the Instructions for Authors (www.plantcell.org) is: Clive Lloyd (clive.lloyd@bbsrc.ac.uk).

[W] Online version contains Web-only data.

www.plantcell.org/cgi/doi/10.1105/tpc.109.069716

some new microtubules do branch, others follow an existing microtubule track.

## RESULTS

### The Emergence of Cortical Microtubules

In this study, *A. thaliana* end-binding protein 1a, AtEB1-GFP, which binds the plus ends of microtubules with high affinity, has been used to see where new comets emerge within the cortical array, something that is not always possible with GFP-tubulin when one microtubule grows along another (Dixit et al., 2006). As well as labeling the plus-end comet, EB1 also labels the shanks of microtubules with lower affinity (as seen in animal cells; Tirnauer et al., 2002), and this sidewall labeling is useful for investigating depolymerization events. Kymographs (a time-distance projection along the axis of the microtubule) were used for analyzing when and where the microtubule comet emerges (Figures 1A to 1C). The origin of a comet on a kymographed microtubule marks the site from which the microtubule evidently grows, and in these *Arabidopsis* plants expressing AtEB1-GFP under the 35S promoter, that site is marked by a focus of EB1. In animal cells, neural precursor cell expressed developmentally downregulated protein 1 (NEDD1), targets the gamma tubulin ring complex to the centrosome (Fant et al., 2009). In plants, NEDD1 decorates the spindle poles of plant cells (Zeng et al., 2009) and during interphase labels cytoplasmic spots associated with cortical microtubules (Motose et al., 2008). We therefore used it as a potential marker of microtubule nucleation sites. Using transient expression in *Nicotiana benthamiana*, in four independent experiments, it was determined that out of 267 foci labeled with red fluorescent protein (RFP)-NEDD1 in epidermal cells, 208 were colabeled with EB1-GFP (see Supplemental Figure 1 online), and it was observed that microtubules emerge from such double-labeled foci (see Supplemental Figure 2 online). It is not possible to conclude whether EB1 is a native component of such foci or is artifactually binding but in this system it clearly marks the sites at which microtubules appear upon the cortex and is exploited here as an expedient marker.

Apart from plus-end comets, foci were mainly distributed along the length of extant microtubules (95%, $n = 321$; five cells), the remainder being found at cortical sites deficient in microtubules (Chan et al., 2003; Shaw et al., 2003). Foci often appeared along growing microtubules (0.43 events/1000 $\mu m^2$/min, SD $\pm$ 0.23; $n$ = six hypocotyls). On time versus distance kymographs, such sites arose as vertical (i.e., stationary) lines upon the sloping trace generated by growing microtubule plus end (Figures 1D to 1F). Such sites either appeared concomitantly with plus-end growth (Figures 1D to 1F) or following growth where the focus is recruited along the shank of a growing microtubule.

Foci marked the site of comet emergence, and it could be seen that they sometimes moved with the microtubule. Although the majority of foci were stationary (90%, 143 foci, $n$ = 158), hence

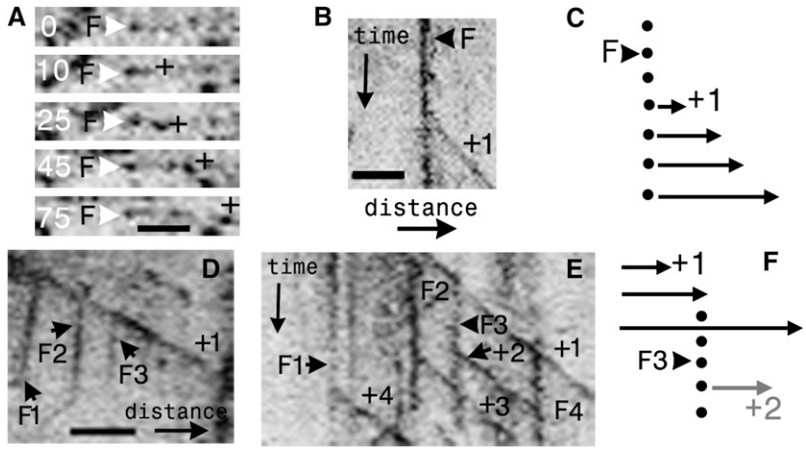


**Figure 1.** Sites of Microtubule Initiation Propagate with Plus-End Growth.

**(A)** Time-lapse series showing initiation and growth of microtubule plus-end comet of AtEB1a-GFP (+) from a cortical focus (F; white arrowhead). Time is indicated in seconds.

**(B)** Kymograph showing a moving EB1 comet, which forms a sloping line (+1), emerging from the vertical line of a stationary focus (F).

**(C)** The diagram of this event shows the growing microtubule (arrow) emerging from a fixed point (circles). The heads of the arrows (EB1 comets) join to trace a sloping line as time moves down the page.

**(D)** Kymograph along the axis of a growing microtubule (+1) as it grows. Multiple foci (F1 to F3) develop along its length, and such foci are seen as stationary vertical lines.

**(E)** A focus (vertical line, F3; arrowhead) that forms along a growing mother microtubule (+1) initiates a new microtubule (+2; arrow). Note that other stationary foci (vertical lines, F1 [arrow] and F2) also initiate plus-end comets (sloping lines +4 and +3, respectively).

**(F)** A diagram of this event shows that a stationary focus (F3, hence the vertical line down the time axis) arises on a growing mother microtubule (+1). A new comet, +2, then forms from that focus.

Bars lengths are as follows: 2 $\mu$m in **(A)**; in **(B)** (bar located in bottom left-hand corner of panel), $x$ axis = 3.1 $\mu$m, and $y$ axis = 78 s; in **(D)** and **(E)**, $x$ axis = 4 $\mu$m, and $y$ axis = 98 s (bar located at the bottom of **[D]**).

forming vertical traces on a kymograph (Figures 1B, 1D, and 1E; see Supplemental Movie 1 online), a minority (10%, 12 foci, $n$ = 158) appeared to track with the depolymerizing ends of microtubules, moving in plus (i.e., moving toward the plus end of its emergent comet) or minus (i.e., moving in the opposite direction prior to comet emergence) directions. Movement toward the plus end of a microtubule was relatively slow, ranging from 0.7 to 2.7 μm/min with an average rate of 1.8 μm/min (SD ± 0.7; $n$ = 15) (see Supplemental Figures 3A to 3D and Supplemental Movie 2 online) similar to the minus-end depolymerization rate calculated for microtubules of hypocotyl cells (Shaw et al., 2003). Movement toward the minus ends of microtubules was more frequent (0.41 [SD ± 0.56] versus 0.14 [SD ± 0.17] events/1000 $\mu m^2$/ min, $n$ = six hypocotyls) and occurred when foci tracked the plus ends of depolymerizing microtubules (see Supplemental Figures 3F and 3G and Supplemental Movie 1 online). The rate varied between 1 and 12 μm/min, with an average of 5.5 μm/min (SD ± 2.3; $n$ = 27). When the minus-end foci reached the minus ends of depolymerizing microtubules, they were observed to exhibit erratic movements, presumably due to their detachment from the cortex. The distribution of these sites, from which comets are seen to emerge using AtEB1-GFP, is consistent with other studies using GFP-tubulin (Murata et al., 2005; Nakamura and Hashimoto, 2009).

In summary, these results indicate that sites at which new comets arise are diffusely distributed at the cell cortex, they are recruited to growing microtubules, and, as previously shown by Chan et al. (2003), they move in a manner that relates to the dynamics of the mother microtubule.

### Branching of Cortical Microtubules Is Directionally Biased

Using GFP-tubulin, Murata et al. (2005) showed that microtubules branch off a mother microtubule at 41.6 ± 8.2°. However, as noted by Dixit et al. (2006), it is difficult to use GFP-tubulin to resolve one microtubule growing along another; hence, the polarity of the mother microtubule can be difficult to determine in such cases, and it may not be clear if a microtubule is branching toward the plus or the minus end of the mother microtubule. AtEB1-GFP allows the direction of branching to be determined, and the branching was only quantified for those cases where the branching microtubule(s) could be clearly seen to originate from the linear, polarized trace generated by the mother microtubule (Figures 2A and 2B). This was also performed for SPR1-GFP, as shown in Supplemental Figure 4 online. Thus, branching angles were measured along the axis of single, rather than antiparallel, microtubules of known polarity.

Figure 2C shows that the outgrowth of new microtubules was highly biased for certain trajectories, relative to the mother microtubule. Broadly consistent with Murata et al. (2005), the bulk of microtubules branched at angles of ±5° to 60° relative to the mother microtubule. Outgrowth of a new EB1 comet showed no significant preference for one side of the mother microtubule over the other ($\chi^2$ test for goodness-of-fit to 1:1 ratio, P = 0.4); Figure 2B shows a projection of branching events occurring on both sides of a mother microtubule. Importantly, our analysis of 230 branching events (54 multievents/136 single: see below) shows that growth is directionally biased since new microtubules grow, albeit with some latitude, in the same direction as the mother microtubule. This is borne out by the fact that the great majority of new microtubules grow toward one end (the plus end) and not both ends of the mother microtubule's axis. This biased distribution underlines the importance of a microtubule polarity marker, since a random assignment of the polarity of mother microtubules would have shown that 50% of the branches grow in the opposite direction (giving extra peaks either side of the minus end of the mother microtubule). Analysis of the branching events (Figure 2C) also revealed that a subtle difference in the variance of angles on the right was significantly greater than the variance on the left (F-test: P = 0.002). Within the predominant plus end–directed splaying sector of ±5° to 60°, proportionately fewer microtubules grew on the right-hand side of the microtubule than the left-hand side (74% versus 85%, respectively). Consequently, the mean angles of branching were also significantly different: 55° on the right-hand side of a bundle versus 44° on the left ($t$ test: P = 0.01).

In summary, there is a strong tendency for new microtubules to branch forward, in the same direction that the mother microtubule grows. Despite the higher cytoplasmic background, this finding was corroborated with GFP-SPR1 under its native promoter (see Supplemental Figure 4 online), where nucleation was also seen to be forward-facing with branches growing to right and left ($n$ = 36).

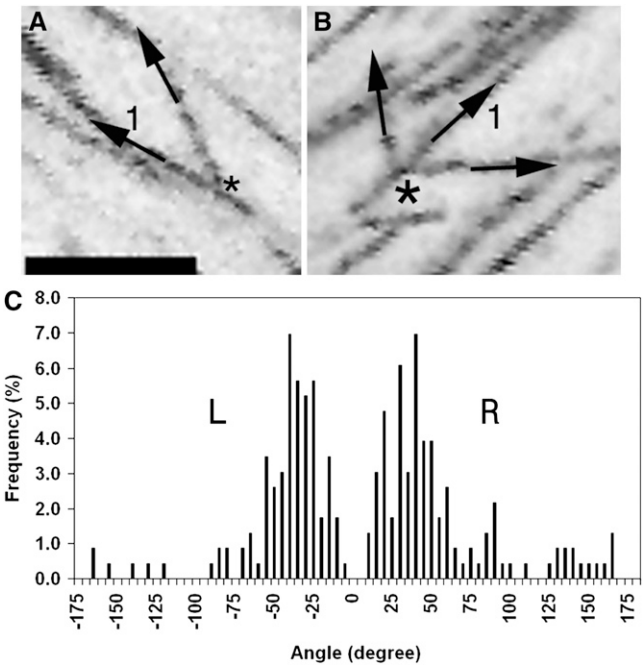


**Figure 2.** Microtubules Branch to Left and Right.

**(A)** Projection showing a microtubule branching to the right of a mother microtubule (1) forming a branchpoint (asterisk).

**(B)** Projection showing microtubules branching either side of a mother microtubule (1) from a branchpoint (asterisk).

**(C)** Analysis of branching angles. Microtubules branch to left or right within a ±5° to 60° splay zone relative to the plus end of the mother microtubule (0°).

Bar in **(A)** = 5 μm for **(A)** and **(B)**.

### A Population of Newly Nucleated Microtubules Grows along the Mother Microtubule

As Murata et al. (2005) noted, the occurrence of branching presents an apparent paradox since microtubules are generally considered to be organized in parallel groups. We therefore examined the possibility that some microtubules are born, unbranched, along the axis of preexisting microtubules as suggested by our previous work (Chan et al., 2007). The sidewall labeling by AtEB1-GFP allows us to distinguish microtubule shrinkage and subsequent rescue from de novo appearance of a microtubule. Nevertheless, to remove any possible confusion with rescue, we only quantified the angles of microtubule emergence at sites where multiple plus-end comets emerged at different angles and, importantly, were coexistent (Figures 3A to 3D; see Supplemental Movies 1 and 2 online). This functional criterion allowed sites of apparent microtubule nucleation (Shaw et al., 2003) to be distinguished from the site of a rescue. Switching from shrinkage to growth would have produced a single comet and not multiple, coexistent comets. Taking Figures 3C and 3D for example, the angle of outgrowth of the EB1 comets labeled +1 and +2 were scored since both originated from the same focus (F) and were coexistent. EB1 comet +3 was not scored since it did not coexist with either of the comets (+1 nor +2) and could therefore have originated from the rescue of comet +2 (at, or close to, the focus). Multiple comet emergence from single foci was a relatively rare event: in a total of 164 events, 87% were single and 13% multiple ($n$ = six hypocotyls). Single comets were seen at a frequency of 1.79 events/1000 $\mu m^2$/min ± 1.21, compared with 0.36 events/1000 $\mu m^2$/ min, SD ± 0.34 ($n$ = six hypocotyls) for multiple emergence.

This analysis of 62 multicomet emergence events revealed that, in addition to branching, a significant proportion (38%, $n$ = 165 microtubules growing from 62 events) of new comets arose upon and followed the mother axis. Of this 38%, 31% grew forward (0°) and 7% backward (180°) with relation to the polarity of the mother microtubule, sharing the preference shown by the branching microtubules for forward growth. It is important to note that de novo emergence is distinct from rescue; in the latter case, kymographic analysis reveals sidewall labeling trailing back to the site from which the comet will regrow, but this is not seen with new initiations (see Supplemental Figure 3B online).

### Some Microtubules Are Nucleated at Cross-Over Points

An alternative location of new microtubules was revealed by movies that showed new EB1 comets arising at sites of

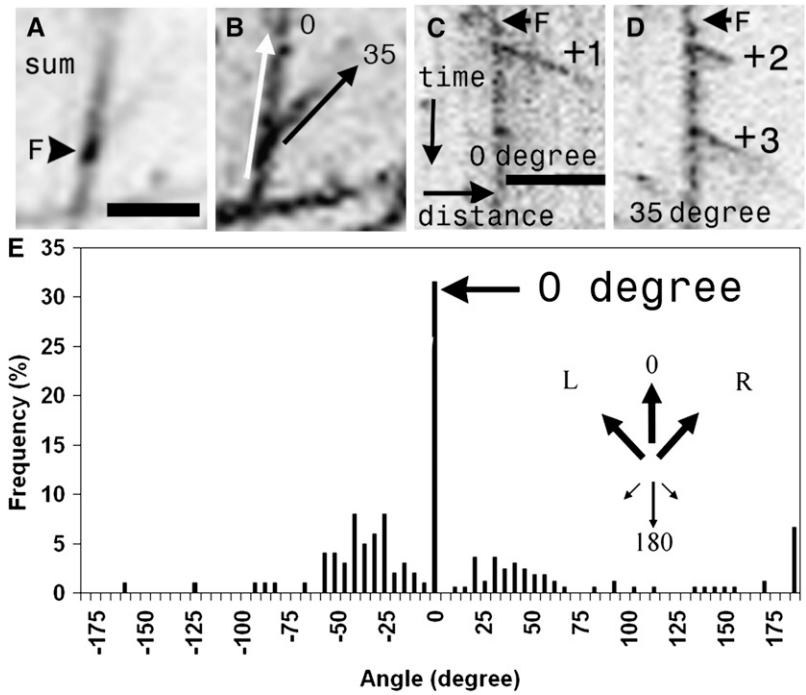


**Figure 3.** Microtubule Initiation at the Cortex Is Directionally Biased.

**(A)** The sum projection of a time-lapse movie shows a microtubule-associated focus (F; arrowhead).
**(B)** The max projection shows that multiple microtubule initiations from the focus in **(A)** result in branching at 35° relative to the mother microtubule (0°).
**(C)** and **(D)** Kymographs along the 0° (**[C]**; white arrow in **[B]**) and 35° (**[D]**; black arrow in **[B]**) axis of this focus reveal a single initiation (+1) along the 0° axis and two initiations along the 35° axis (+2 and +3). Note, comets +1 and +2 are initiated simultaneously.
**(E)** Angles of microtubule emergence from cortical foci ($n$ = 165). The major angle of 0° (arrows) denotes growth along the mother microtubule, toward its plus end. Inset: arrow diagram summarizing the directional bias of nucleation.
Bar in **(A)** = 2 μm for **(A)** and **(B)**; bar in **(C)** (same as for **[D]**): $x$ axis = 4 μm, and $y$ axis = 98 s.

microtubule–microtubule interaction, in particular where growing microtubules crossed paths (Figures 4A to 4D; see Supplemental Movies 3 and 4 online). A quantitative analysis of 214 microtubule–microtubule encounters showed that 18.2% resulted in emergence of new comets from the cross-over point. Wightman and Turner (2007) first noted that severance of the crossing microtubule, accompanied by shrinkage of the new lagging end, provides a mechanism for the removal of unaligned microtubules. Here, it is shown that new microtubule plus-end comets appear at these junctions (0.65 events/1000 $\mu m^2$/min, SD $\pm$ 0.2, $n$ = six hypocotyls), representing 23% (51 events) of all emergent comets (i.e., including single and multiple comets originating from foci, $n$ = 214). After crossing paths, the emergence of single (48 events) as well as multiple (three events) microtubule plus-end comets was observed within a mean time of 55 s ($n$ = 56; SD $\pm$ 32). Notably, the majority of plus ends appearing at crossroads followed paths delineated by one or other of the crossing microtubules (77%, 43 microtubules: 50% along the obstructing and 27% along the crossing) instead of initiating new trajectories (23%, 13 microtubules). Analysis of the EB1 data suggested no strict correlation between the angle at which microtubules crossed over and the path subsequently taken by the newly initiated comet (i.e., whether it grew either way along the axis of the obstructing or the crossing microtubule or in a new orientation).

We also observed the appearance of new microtubules after cross-over in seedlings expressing GFP-tubulin, especially when growth occurred at a divergent angle to the junction's axes (see Supplemental Movie 5 online). This was further confirmed with GFP-SPR1 under its native promoter (Sedbrook et al., 2004) (Figure 4K), illustrating that the appearance of new plus ends at crossroads is not restricted to cells expressing EB1-GFP. Out of 36 events, 31 led to the emergence of a single comet and five were multiple events. Fifteen new comets grew along the path of the crossing microtubule, another 13 along the obstructing, and 13 at divergent angles.

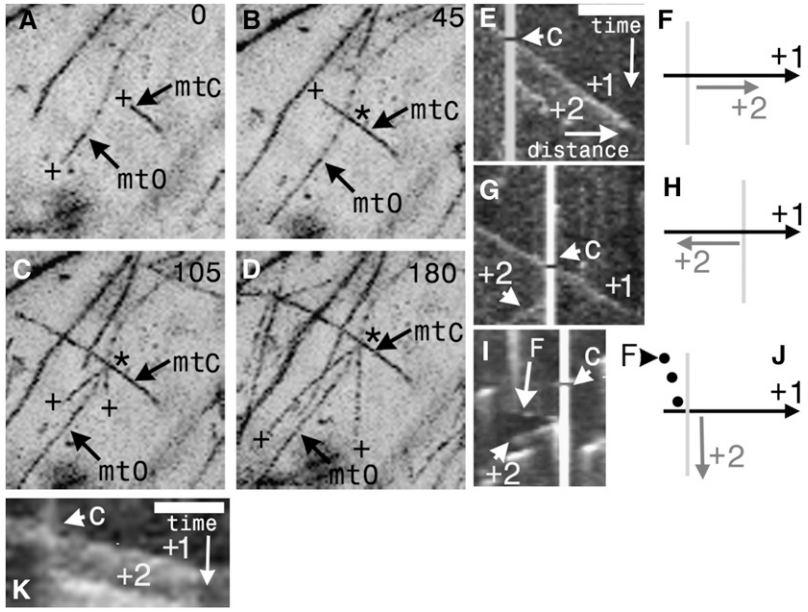


**Figure 4.** Microtubules Initiate at Microtubule Cross-Over Junctions.

**(A)** to **(D)** A time-lapse series showing a crossing microtubule (mtC) grow and cross-over an obstructing microtubule (mtO). Two new microtubules (both plus ends marked + in **[C]** and **[D]**) are then initiated at divergent angles from the junction (asterisks).

**(E)** to **(K)** Microtubule emergence along the axis of crossroad junctions.

**(E)** Kymograph along the axis of an incoming microtubule that crosses the path (arrowhead, C) of an obstructing microtubule (marked by the vertical white line). A new, coexistent microtubule (+2) is initiated at the cross-over point and grows in the same direction as the crossing microtubule.

**(F)** The accompanying diagram shows the new +2 microtubule emerge from the cross-over point.

**(G)** Kymograph along the axis of an incoming microtubule that crosses the path (arrowhead, C) of an obstructing microtubule (marked by the vertical white line). A new, coexistent microtubule (+2) is initiated at the cross-over point and here it grows in the opposite direction to the crossing microtubule.

**(H)** The accompanying diagram shows the nascent microtubule (+2) grow in the opposite direction to the previous example.

**(I)** Kymograph along the axis of an obstructing microtubule during microtubule cross-over. The cross-over point is marked by the vertical white line and the time of cross-over by the arrowhead (C). The backward-sloping and dotted trace of a focus (F) tracking with a depolymerizing microtubule leads back to the cross-over point, from which a comet is subsequently initiated (+2, arrowhead).

**(J)** The accompanying diagram shows a new microtubule (+2) emerging from the cross-over point.

**(K)** A microtubule labeled with SPR1-GFP showing the same behavior as **(E)** with EB1-GFP. A microtubule (+1) crosses (C) the path of another microtubule; a new microtubule (+2) is initiated at the cross-over point and grows in the same direction as the crossing microtubule.

Bar = 7 $\mu$m for **(A)** to **(D)**; for **(E)**, **(G)**, and **(I)** (bar located in the top right-hand corner of **[E]**): $x$ axis = 5 $\mu$m, and $y$ axis = 128 s. **(A)** to **(D)** were obtained from maximum intensity projections.

While rescue can account for the appearance of some new microtubules at crossroads, it cannot explain those cases where a new comet diverges at an angle from the crossroad's axes. Nevertheless, we only scored new microtubules that were coexistent with the crossing microtubule. This is illustrated in kymographs prepared along the axis of the crossing microtubule (Figures 4E to 4H) in which the emergent comets appear while the crossing microtubule maintains steady growth, undergoing neither catastrophe nor rescue (i.e., 0° and 180°; Figures 4E and 4G, respectively). Of further note, the crossing microtubule was always marked by a single comet that moved into virgin territory unoccupied by other microtubules and hence was marking a single end.

Kymographs, which trace the origins of comets that appear along the axis of the obstructing microtubule, revealed trails generated by foci tracking back to the cross-over point (seven examples, Figures 4I and 4J). Similar trails of foci moving with depolymerizing microtubules were described above (see Supplemental Figure 3 and Supplemental Movie 1 online). Since foci were observed to move with the depolymerizing ends of microtubules and stop at crossroads (Figure 4I), intersections could serve as anchor points for the deposition of nucleating material that moves with microtubule dynamics. Alternatively, crossroads might act as stable points from which microtubules are rescued independent of any focus. However, the fact that there are examples where coexistent comets emerge at a divergent angle to the junction or along the same axis as the crossing microtubule reinforces the idea that new comets do emerge at crossroads, and they are not solely sites from where shrinking ends are rescued.

Evidence of severing following microtubule cross-over was also detected by kymographic analysis using EB1-GFP (Figures 5A and 5B) (0.42 events/1000 $\mu m^2$/min, SD $\pm$ 0.34, $n$ = 6 hypocotyls), in which the posterior portion of the severed microtubule underwent catastrophe, whereas the anterior portion moved by hybrid treadmilling (Shaw et al., 2003). This phenomenon was also readily observed in hypocotyl cells expressing GFP-tubulin (see Supplemental Movie 6 online). Wightman and Turner (2007) reported severing of the crossing microtubule, and our movies show that the obstructing microtubule can also be cut following crossover (see Supplemental Movie 7 online). Severing was also observed to occur at foci undergoing multiple plus-end outgrowth (Figures 5B to 5D).

In summary, cross-over results in the emergence of new comets that coexist with the crossing microtubule. Because new comets tend to follow one of the crossing microtubules this behavior represents another opportunity to reinforce the preexisting microtubule orientation and to promote bundling. This phenomenon was also observed in seedlings expressing GFP-tubulin and was confirmed with GFP-SPR1 under its native promoter (Sedbrook et al., 2004).

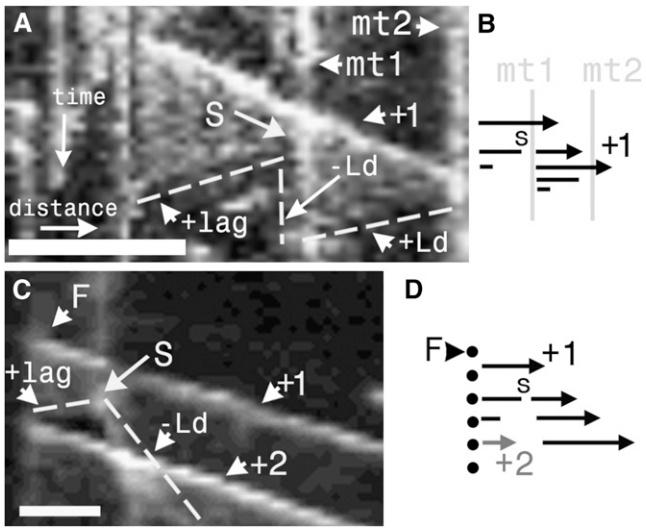


**Figure 5.** Kymographs of Microtubule Severing.

**(A)** Kymograph along the axis of a growing microtubule (+1) that is severed (S) as it crosses an obstructing bundle (vertical trace, mt1). Reading the subsequent timeline down the page, severing then generates a sawtooth pattern (dashed line) traced by the lower-affinity AtEB1a-GFP labeling of microtubule sidewalls. Sawtooth patterns arise from the different behaviors exhibited by the cut ends: the exposed plus end of a lagging microtubule undergoes relatively rapid depolymerization (making a backward-sloping line: +lag), whereas the newly exposed minus end of the leading portion remains fairly static (vertical line: −Ld). The growing plus end at the far right of +1 undergoes depolymerization upon collision with another obstructing microtubule (mt2) at the edge of the kymograph, generating another backward sloping line (+Ld) terminating at its recently severed minus end. Note that the –Ld trace coincides with the vertical trace generated by mt1.

**(B)** The accompanying diagram shows a microtubule (arrow) crossing mt1 and then severing (S). The minus end to the left then shrinks, while the arrowed plus end grows until it collides with mt2 (denoted by the vertical line down the right-hand side of the kymograph) and then shrinks.

**(C)** A microtubule (+1) is severed (S) soon after its initiation from a focus **(F)**. The newly exposed plus end of the lagging microtubule depolymerizes back to the focus (short dashed line, +lag), from which another comet (+2) is initiated and which is coexistent with microtubule (+1). –Ld marks the minus end of the leading portion of the severed microtubule.

**(D)** The accompanying diagram shows a severance (S), the shrinkage of the lagging end back to the focus, and the emergence of a new microtubule (+2).

Bars are as follows: in **(A)**, $x$ axis = 5 $\mu$m, and $y$ axis = 95 s; in **(B)**, $x$ axis = 1.1 $\mu$m, and $y$ axis = 51 s.

## DISCUSSION

In a previous time-lapse study, the cortical microtubule arrays of growing hypocotyl cells expressing AtEB1a-GFP were observed to display polarized behavior (Chan et al., 2007). The microtubule arrays were composed of domains (patches of bundles) in which the overwhelming majority of microtubules grew in the same direction. A cell typically contained several of these domains distributed across its outer epidermal surface and the independent movements of domains in curved paths, in the direction of their plus end, generated the rotation of the entire cortical array. At higher resolution, polarized domains were seen to be composed of branching bundles along which successive comets

flowed along the same axes and combined to form a fluid network. Now, these observations show that the emergence of EB1 and SPR1 comets is directionally biased; the majority of trajectories follow a narrow range of branching angles that are predominantly forward-facing (i.e., toward the plus end of the mother microtubule), which helps to explain the existence of polarized domains and their mobile nature.

### Branching of Nascent Microtubules Is Directionally Biased

Branching from individual microtubules has been described in algae by following recovery from the drug-induced disassembly of cortical microtubules (Wasteneys and Williamson, 1989). From this, a branching-cluster model was proposed in which microtubule-initiating factors move along existing microtubule tracks and nucleate the assembly of new microtubules, which diverge from extant microtubules at an acute angle. Branching was subsequently observed in the higher plant *A. thaliana* (Chan et al., 2003); it was also seen in tobacco suspension cells (Murata et al., 2005) where branching occurred at an angle of 45° and was shown to be dependent upon the recruitment of γ-tubulin. However, the use of a plus-end marker in this study provides important additional information on the polarity of the branching microtubule relative to the mother, with implications for the observed flow of the entire cortical array and its constituent tracks or bundles (Chan et al., 2007). Because microtubules of known polarity can be seen moving along another of known polarity, it is possible to conclude that branching is directionally biased. That is, microtubules tend strongly to branch in the general direction of the mother microtubule's plus end(s), with very few growing backward along the axis. According to Dixit and Cyr (2004), microtubules that branch from one track at <40° tend to converge (zipper) with parallel microtubules; hence, our observation that microtubules tend to branch off mother microtubules in a plus-end direction, and in a splay zone of ±5° to 60°, provides an explanation for the movement of microtubules from one parallel bundle to another while maintaining the plus-end momentum of neighboring bundles in the polarized domain (Chan et al., 2007). Such branching from one bundle to the next would ensure that zippering of microtubules colliding at shallow angles would not inexorably form a superbundle. Branching might also account for the tendency of domains to move laterally over the longer time period, giving rise to rotation.

### Microtubules Emerge along Existing Microtubules

In their elegant study, Murata et al. (2005) drew attention to the paradox that nascent microtubules branch off the mother and yet the cortical array is composed of essentially parallel elements. Zippering of the branching microtubule with an adjacent parallel microtubule (Dixit and Cyr, 2004) provides one explanation for restoration of overall parallelism, but our results suggest additional mechanisms. When microtubules are labeled along their length by GFP-tubulin, it is difficult to see microtubules moving in parallel along one another (Dixit et al., 2006), as we confirmed. Present observations with EB1-GFP reveal that in addition to branching, a significant proportion of the newly born microtubules arise along the preexisting axis, and this occurs in two different locations. The first location is at sites of apparent microtubule nucleation from which multiple, coexistent EB1 comets emerge. The appearance of more than one branching comet from the same point is not explained by the rescue of a shrinking end and is consistent with de novo initiation. Parallel organization (i.e., bundling) can be imposed upon preexisting discordant microtubules in the postnucleation event of zippering. However, the fact that we observe, from apparent sites of nucleation, nascent microtubules growing along the axis of the mother, suggests that coalignment can be part of the initiation event such that bundles can be instantly formed. One possibility for the plus-end bias in the outgrowth of new microtubules is that nucleating material is sterically constrained upon the mother whose own polarity (and perhaps even chirality) may be part of the directional information. Immediate bundling, together with zippering at a later stage, helps to explain the long-term persistence of microtubule bundles along which successive comets grow (Chan et al., 2007). The small percentage of newly nucleated microtubules growing backward along the mother microtubule could represent inherent variability in the angle of nucleation. Alternatively, because the percentage of microtubules growing forward is so overwhelmingly high, this minority population could represent experimental error (e.g., inclusion of some bundled antiparallel microtubules such that apparently backward-directed offshoots are in reality growing in the forward direction of one of the microtubules).

The second location where new microtubules can be seen to grow along an existing axis is at crossroads following microtubule crossover. Our observations indicate that there is a strong tendency for the new comets that arise at cross-overs to grow along one of the crossing microtubules. In addition to AtEB1-GFP, this has been observed with 35S:GFP-tubulin and SPR1-GFP under its own promoter. There are three explanations for the emergence of new microtubules at crossroads. First, nucleating material may be deposited at crossroads by growing or shrinking microtubules or when recruited from the cytoplasm to this physical junction. Consistent with crossroads as sites for new growth, we have observed comets (some of them multiple) to be initiated in new trajectories, including the opposite direction (i.e., 180°) to the incoming crossing microtubule (e.g., Figure 4B). Second, it is formally possible that cross-overs could coincide with preexisting sites of microtubule initiation. Third, the appearance of new plus ends may result from straightforward severing at crossroads as first reported by Wightman and Turner (2007). Those authors reported severing of the crossing microtubule, and here we show that the obstructing microtubule can also be cut following cross-over. This kind of breakage could result from the physical collision of microtubules or from the action of severing proteins, such as katanin, carried at the plus tip (Stoppin-Mellet et al., 2006).

In summary, the tendency of newly nucleated microtubules to follow the mother microtubule or, if arising at crossroads, to follow one of the crossing microtubules, helps explain the paradoxical finding that cortical microtubules form bundles despite their tendency to branch. Kymographs indicate several activities may contribute toward generating new microtubule comets at these sites. The tendency for new comets to be biased in the general direction of the mother microtubule's plus

end also explains our previous observation (Chan et al., 2007) that microtubules flow between adjacent bundles, with groups or domains of adjacent bundles sharing the general direction of flow.

## METHODS

### Plant Material

*Arabidopsis thaliana* plants expressing 35S:AtEB1a-GFP and 35S:GFP-TUA6 are described by Ueda et al. (1999) and Chan et al. (2005). Plants expressing 35S:AtEB1a-GFP were selected that only displayed low levels of fluorescence and exhibited growth characteristics indistinguishable from controls. GFP-SPR1 is described by Sedbrook et al. (2004) and RFP-NEDD1 by Motose et al. (2008). Binary constructs transformed in agrobacteria (LBA4404 strain) were grown for 12 to 24 h at 28°C in 5 mL Luria-Bertani medium containing selective antibiotics, resuspended in water (at a final $OD_{600}$ = 0.2), and syringe-infiltrated into leaves. At 36 to 46 h after infiltration, the plants were observed by fluorescence microscopy. *Arabidopsis* seedlings were grown on plates containing 3% (w/v) Phytagel (Sigma-Aldrich), 0.5% (w/v) sucrose (Sigma-Aldrich), and 0.43% (w/v) Murashige and Skoog powdered medium (Sigma-Aldrich), with macro- and micro-elements (Duchefa). Plates were incubated for 2 d at 4°C and then transferred to the growth room at 22°C under continuous lighting. Seedlings were imaged at intervals over 2 to 5 d, over the period we previously showed the plants are growing (Chan et al., 2007). All data therefore refer specifically to microtubules beneath the outer epidermal walls of light-grown *Arabidopsis* hypocotyl epidermal cells. The reported behaviors were observed in cells at the top, middle, and base of the hypocotyl but were easier to observe at the base where the microtubules were less dense.

### Confocal Imaging and Image Analysis

Images were acquired using Bio-Rad MRC 1024 and Zeiss LSM 510 Meta confocal microscopes. Time-lapse images were acquired at 5-s intervals for up to 10 min. Microtubule dynamics were measured from kymographs (line montages in time along the axis of microtubule growth). Kymographs were constructed using the reslice tool of ImageJ (http://reb.info.nih.gov/ij/). Explanatory note on interpretation of kymographs: a line is drawn along the trajectory of a growing microtubule and this is retraced at intervals to produce a stack. As the microtubule grows from left to right, its plus-end comet is displaced down the page, tracing an oblique line. The slope of this resulting oblique line gives the rate of movement, and the direction of slope gives the direction of movement. An immobile point on the microtubule will generate a vertical line.

Microtubule angles were measured from time projections of time-lapse images. Max projection refers to projection of the maximum pixel intensities of the z-stack/time-lapse movie at each x,y location of the image. Sum projection refers to the sum of pixel intensities over the z-stack/time-lapse movie at each x,y location of the image. Branching angles were measured in a clockwise direction relative to the plus end of the mother microtubule. Angles of microtubule cross-over/encounter were measured in a clockwise direction relative to the crossing microtubule since the polarity of this microtubule was always known.

### Accession Numbers

Sequence data from this article can be found in the Arabidopsis Genome Initiative or GenBank/EMBL databases under the following accession numbers: AtEB1a, At3g47690; TUA6, At4g14960 ; SPR1, At2g03680; and NEDD1, At5g05970.

### Supplemental Data

The following materials are available in the online version of this article.

**Supplemental Figure 1.** AtEB1a-GFP Foci Colocalize with Spots of NEDD1-RFP along Microtubules.

**Supplemental Figure 2.** Microtubules Emerge from Foci Double-Labeled with AtEB1a-GFP and NEDD1-RFP.

**Supplemental Figure 3.** Plus- and Minus-End Directed Movements of Cortical Sites of Microtubule Emergence.

**Supplemental. Figure 4.** Microtubules Branch to Left and Right in SPR1:SPR1-GFP Plants.

**Supplemental Movie 1.** Emergence of Microtubules and Behavior of Cortical Foci Labeled by AtEB1a-GFP in an *Arabidopsis* Hypocotyl Cell.

**Supplemental Movie 2.** Emergence of Microtubules and Behavior of Cortical Foci Labeled by AtEB1a-GFP in an *Arabidopsis* Hypocotyl Cell.

**Supplemental Movie 3.** Emergence of Microtubules at a Crossroad Junction in a Hypocotyl Cell Expressing AtEB1a-GFP.

**Supplemental Movie 4.** Emergence of Microtubules at a Crossroad Junction in a Hypocotyl Cell Expressing AtEB1a-GFP.

**Supplemental Movie 5**. Microtubule Growth at a Crossroad Junction in a Hypocotyl Cell Expressing GFP-Tubulin.

**Supplemental Movie 6.** Severing of Microtubules at Crossroad Junctions in a Hypocotyl Cell Expressing GFP-Tubulin.

**Supplemental Movie 7.** Microtubule Severing and Growth at Crossroad Junctions in a Hypocotyl Cell Expressing GFP-Tubulin.

## ACKNOWLEDGMENTS

This work was supported by a grant-in-aid by the Biotechnology and Biological Sciences Research Council to the John Innes Centre. We thank J. Brown for help with statistical tests. We also thank T. Hashimoto, V. Kirik, H. Motose, and J. Sedbrook for providing constructs.

Received June 30, 2009; revised August 5, 2009; accepted August 13, 2009; published August 25, 2009.

## REFERENCES

**Chan, J., Calder, G., Fox, S., and Lloyd, C.** (2005). Localization of the end-binding protein EB1 reveals alternative pathways of spindle development in *Arabidopsis* suspension cells. Plant Cell **17:** 1737–1748.

**Chan, J., Calder, G.M., Doonan, J.H., and Lloyd, C.W.** (2003). EB1 reveals mobile microtubule nucleation sites in Arabidopsis. Nat. Cell Biol. **5:** 967–971.

**Chan, J., Calder, G.M., Fox, S., and Lloyd, C.W.** (2007). The cortical microtubule array undergoes rotary movements in Arabidopsis hypocotyl epidermal cells. Nat. Cell Biol. **9:** 171–175.

**Dixit, R., Chang, E., and Cyr, R.** (2006). Establishment of polarity during organization of the acentrosomal plant cortical microtubule array. Mol. Biol. Cell **17:** 1298–1305.

**Dixit, R., and Cyr, R.** (2004). Encounters between dynamic cortical microtubules promote ordering of the cortical array through angle-dependent modifications of microtubule behavior. Plant Cell **16:** 3274–3284.

**Dhonukshe, P., Mathur, J., Hulskamp, M., and Gadella, T.W., Jr.** (2005). Microtubule plus-ends reveal essential links between

intracellular polarization and localized modulation of endocytosis during division-plane establishment in plant cells. BMC Biol. **3:** 11.

**Fant, X., Gnadt, N., Haren, L., and Merdes, A.** (2009). Stability of the small gamma-tubulin complex requires HCA66, a protein of the centrosome and the nucleolus. J. Cell Sci. **122:** 1134–1144.

**Giddings, T.H., and Staehelin, A.** (1991). Microtubule-mediated control of microfibril deposition: A re-examination of the hypothesis. In The Cytoskeletal Basis of Plant Growth and Form, C.W. Lloyd, ed (London: Academic Press), pp. 85–99.

**Hardham, A.R., and Gunning, B.E.S.** (1978). Structure of cortical microtubule arrays in plant cells. J. Cell Biol. **77:** 14–34.

**Hejnowicz, Z.** (2005). Autonomous changes in the orientation of cortical microtubules underlying the helicoidal cell wall of the sunflower hypocotyl epidermis: Spatial variation translated into temporal changes. Protoplasma **225:** 243–256.

**Lancelle, S.A., Callham, D.A., and Hepler, P.K.** (1986). A method for rapid freeze fixation of plant cells. Protoplasma **131:** 153–165.

**Motose, H., Tominaga, R., Wada, T., Sugiyama, M., and Watanabe, Y.** (2008). A NIMA-related protein kinase suppresses ectopic growth of epidermal cells through its kinase activity and the association with microtubules. Plant J. **54:** 829–844.

**Murata, T., Sonobe, S., Baskin, T.I., Hyodo, S., Hasezawa, S., Nagata, T., Horio, T., and Hasebe, M.** (2005). Microtubule-dependent microtubule nucleation based on recruitment of gamma-tubulin in higher plants. Nat. Cell Biol. **7:** 961–968.

**Nakamura, M., and Hashimoto, T.** (2009). A mutation in the Arabidopsis gamma-tubulin-containing complex causes helical growth and abnormal microtubule branching. J. Cell Sci. **122:** 2208–2217.

**Paredez, A.R., Somerville, C.R., and Ehrhardt, D.W.** (2006). Visualization of cellulose synthase demonstrates functional association with microtubules. Science **312:** 1491–1495.

**Refrégier, G., Pelletire, S., Jaillard, D., and Höfte, H.** (2004). Interaction between wall deposition and cell elongation in dark-grown hypocotyl cells in Arabidopsis. Plant Physiol. **135:** 1–10.

**Sedbrook, J.C., Ehrhardt, D.W., Fisher, S.E., Scheible, W.R., and Somerville, C.R.** (2004). The *Arabidopsis* sku6/spiral1 gene encodes a plus end-localized microtubule-interacting protein involved in directional cell expansion. Plant Cell **16:** 1506–1520.

**Shaw, S.L., Kamyar, R., and Ehrhardt, D.W.** (2003). Sustained microtubule treadmilling in Arabidopsis cortical arrays. Science **300:** 1715–1718.

**Stoppin-Mellet, V., Gaillard, J., and Vantard, M.** (2006). Katanin's severing favors bundling of cortical microtubules. Plant J. **46:** 1009–1017.

**Sugimoto, K., Williamson, R.E., and Wasteneys, G.O.** (2007). New techniques enable comparative analysis of microtubule orientation, wall texture, and growth rate in intact roots of Arabidopsis. Plant Physiol. **124:** 1493–1506.

**Timmers, A.C.J., Vallotton, P., Heym, C., and Menzel, D.** (2007). Microtubule dynamics in root hairs of *Medicago truncatula.* Eur. J. Cell Biol. **86:** 69–83.

**Tirnauer, J.S., Grego, S., Salmon, E.D., and Mitchison, T.J.** (2002). EB1-microtubule interactions in Xenopus egg extracts: Role of EB1 in microtubule stabilization and mechanisms of targeting to microtubules. Mol. Biol. Cell **13:** 3614–3626.

**Ueda, K., Matsuyama, T., and Hashimoto, T.** (1999). Visualization of microtubules in living cells of transgenic *Arabidopsis thaliana*. Protoplasma **206:** 201–206.

**Wasteneys, G.O., and Williamson, R.E.** (1989). Reassembly of microtubules in *Nitella tasmanica*: Assembly of cortical microtubules in branching clusters and its relevance to steady-state microtubule assembly. J. Cell Sci. **93:** 705–714.

**Wightman, R., and Turner, S.R.** (2007). Severing at sites of microtubule crossover contributes to microtubule alignment in cortical arrays. Plant J. **52:** 742–751.

**Zeng, C.J., Lee, Y.R., and Liu, B.** (2009). The WD40 repeat protein NEDD1 functions in microtubule organization during cell division in *Arabidopsis thaliana*. Plant Cell **21:** 1129–1140.